Integrative Modeling of Bacterial H2O2 Stress Responses

Chen Liao

February 13, 2019

1 Background knowledge

Reactive oxygen species (ROS) such as superoxide, hydrogen peroxide (H2O2), and hydroxyl radical, can be produced by intracellular aerobic respiration and/or environments. They are toxic to bacterial cells, leading to loss of fitness, including high mutation rates, growth defects, and even cell death. Biochemically, there are two basic classes of H2O2-degrading proteins

1. Catalase: $2H_2O_2 \rightarrow O_2 + 2H_2O$
2. Peroxidases: $RH_2 + H_2O_2 \rightarrow R + 2H_2O$

The electron source of catalase is from H2O2 itself and no exogenous electron source is needed. However, peroxidases can differ in their electron donors (i.e., RH_2), which could be glutathione, thioredoxins, NAD(P)H, cytochrome *c*, dyes and other unknowns.

Catalases rely on iron or manganese so they fall into two categories: heme (an iron-containing compound) calatases and non-heme catalases (or manganese). Catalases with only catalatic activity are called mono-functional catalases, and those with both catalatic activity and peroxidatic activities are referred to as bifunctional catalases or catalase-peroxidases. The activity of catalase-peroxidases is low (ca. 1% of the maximum catalase activity) and thus seems unlikely to be an important contributor to H2O2 degradation.

Peroxidases also fall into two categories: thiol (i.e., RSH)-based peroxidases (peroxiredoxins; abbr. Prx) and non-thiol peroxidases. All peroxiredoxins contain a conserved cysteine that reacts with H2O2 and forms a disulfiide before getting reduced back to free thiol. Depending on the variations in the mechanisms of thiol regeneration, peroxidases can be further calssfied into four groups: alkylhydroperoxide reductases (AhpCF), thiol glutathione peroxidase (Tpx), bacterioferritin comigratory protein (BCP), and glutathione peroxidase (Gpx).

1 *Escherichia coli*

Most of the following information about *E. coli* antioxidant systems come from a review paper [1]. *E. coli* has at least 9 enzymes that have been proposed to be calatases or peroxidases. The major H2O2 scavenging enzyme is Ahp (alkyl hydroperoxide reductase) [2], which consists of two subunits: the small subunit (AhpC), which reduces organic peroxides to their corresponding alcohols, and the large subunit (AhpF), which is involved in the regeneration of oxidized AhpC. AhpF needs NAD(P)H as an electron donor: electron movement within AhpF occurs from NAD(P)H to FAD, from FAD to a C345/C348 thiol/disulfide center, and from thiols to the N-terminal redox-active center (C129/C132). Therefore, Ahp has limited activity under conditions when reducing power is limited (e.g., nutrient starvation).

In the meanwhile, *E. coli* contains two catalases, HPI (hydroperoxidase I, encoded by *katG*) and HPII (hydroperoxidase II, encoded by *katE*). Despite the key role of Ahp, catalase still has an important role in wild-type cells, because the activity of Ahp is saturated at a low concentration of H2O2. In contrast, catalase has a high Km, and it therefore becomes the predominant scavenger when H2O2 concentrations are high. In addition, catalases provide protection even in energy-depleted cells.

When the entry rate of H2O2 is high, basal level defense is inadequate and adaptive response is needed. HPI is transcriptionally induced during the lag [3]/log phase in response to low concentrations of H2O2 and this induction requires the transcriptional regulator, OxyR, which also induces *ahpC*. A key cysteine residue of the OxyR protein is oxidized by H2O2, triggering conformational change from an inactive form (i.e., reduced state) to an active form (oxidized state). The oxidized OxyR then binds to the promoter regions of many genes on the *oxyR* regulon. OxyR positively controls genes for peroxide detoxification, such as catalase and peroxiredoxin (katG, ahpCF), Fe-storage miniferritin (dps), glutaredoxin, thioredoxin and glutathione reductase (grxA, trxC, gor), sulfenic acid oxidoreductase (dsbG), ferric uptake regulator (fur), Fe-S-cluster assembly machinery (sufABCDE), ferrochelatase (hemH), manganese import (mntH) and the small RNA (oxyS) [4]. OxyR negatively regulates its own expression and that of the genes for the ferric ion reductase (fhuF), the outer membrane protein (flu), the mannonate hydrolase (uxuAB) and gluconate permease (gntP) [4]. OxyR is regenerated by the glutaredoxin/GSH/Gor system upon return to non-stress conditions. In contrast to HPI and Ahp, HPII is induced at the transition from exponential phase to stationary phase by RpoS and its induction is OxyR-independent. Mutatino in HPII did not affect the log-phase growth phenotype even in strains lacking HPI and/or Ahp [2].

Other peroxidases seem to play other functions than H2O2-degradation *in vivo*, although their activity has been demonstrated. For example, the *tpx* mutant did not show any phenotype under aerobic growth, while it is more sensitive to organic hydroperoxides. Deletion of *btuE* (Gpx) also does not create sensitivity to H2O2, while the mutant is more sensitive to paraquat and tellurite. In addition, the *E. coli* btuE gene is not induced during H2O2 stress and overexpressing of this gene does not confer protection for cells lacking other antioxidant enzymes.

2 *Pseudomonas aeruginosa*

KatA is the major catalase in *P. aeruginosa* whose expression is constitutively highly in all phases of growth (high basal) but increased upon stationary growth phase and H2O2 treatment [5]. It is highly stable and can be found in the extracellular milieu, which ensures the survival of *P. aeruginosa* cells in its biofilm state. Other typical antioxidant enzymes for the defense against H2O2 challenges include catalases (KatB and KatE) andalkyl hydroperoxide-reducing proteins (AhpB, AhpC, and Ohr). The *katA*, *katB*, *ahpB*, and *ahpCF* genes are positively regulated by OxyR in response to H2O2 and menadione or paraquat (PQ) treatments. KatA was also found to be regulated by quorum sensing signals [6]. Recently, it was reported that KatE was induced by high temperature and requires the disulfide bond formation system for its activity.

It was also found that inactivation of the *P. aeruginosa* stringent response (SR), a starvation stress response controlled by the alarmone (p)ppGpp, caused impaired antioxidant defenses and antibiotic tolerance. Upon amino acid starvation, induction of the SR upregulated catalase activity. Full expression of *katA* and *katB* also required the SR, and this regulation occurred through both RpoS-independent and RpoS-dependent mechanisms. Overexpression of *katA* was sufficient to restore H2O2 tolerance and to partially rescue the antibiotic tolerance of SR cells.

2 Modeling H2O2 diffusion, production and decomposition

Fig. 1 shows the schematic diagram of H2O2 diffusion, production and decomposition.

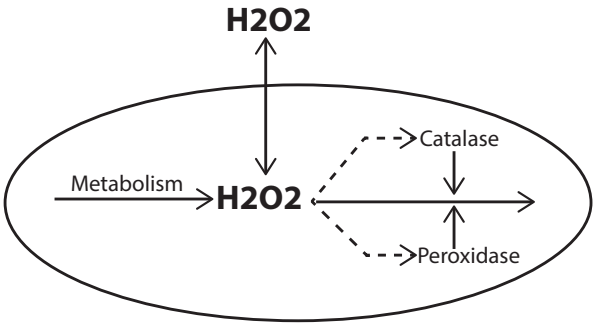

Fig. 1: Schematic diagram of H2O2 reactions.

1 Unregulated model (constant Ahp and KatG)

We assume that extracellular H2O2 ($[H_o]$) is a constant and intracellular H2O2 ($[H_i]$) is produced at a constant rate. Two enzymes, Ahp and KatG, are considered but their enzyme concentrations are assumed constant as well. In *E. coli*, Ahp becomes saturated at a low concentration of H2O2 (low K_m), while catalase has a high K_m. Therefore, decomposition of H2O2 by Ahp and catalase are modelled using Michaelis-Menten and first-order equation respectively. The model for intracellular H2O2 at steady state is

$$\frac{dH_i}{dt} = k_{met} + ([H_o] - [H_i])PA - k_{cat}[H_i] - \frac{k_{ahp}[H_i]}{K_{m,ahp} + [H_i]} \tag{1}$$

where the four terms represent intracellular production rate (k_{met}), diffusion based exchange, decomposition by catalase and decomposition by Ahp respectively. P is permeability coefficient and A is the surface area of the membrane. k_{cat} and k_{ahp} are the maximum decomposition rates by catalase and Ahp respectively. At steady state, we can solve $[H_i]$ as a function of $[H_o]$

$$[H_i] = \frac{-\Delta + \sqrt{\Delta^2 + 4K_{m,ahp}(PA + k_{cat})(k_{met} + [H_o]PA)}}{2(PA + k_{cat})} \tag{2}$$

$$\Delta = K_{m,ahp}PA + K_{m,ahp}k_{cat} - [H_o]PA - k_{met} + k_{ahp} \tag{3}$$

The following parameter values are collected from Seaver and Imlay [7] for *E. coli* cells: $P = 1.6 \times 10^{-3}\ cm/s$, $A = 1.41 \times 10^{-7}\ cm^2$, $k_{met} = 4.5 \times 10^{-20}\ mol/s$, $k_{cat} = 2.7 \times 10^{-13}\ L/s$, $k_{ahp} = 2.1 \times 10^{-18}\ mol/s$, $K_{m,ahp} = 1.2 \times 10^{-6}\ M$. See Fig. 2 for simulated $[H_o]/[H_i]$ ratio for wild-type cell, Catalase mutant, Ahp mutant, and double mutant. Using this set of parameters, the intracellular H2O2 concentration can be as low as 10 fold less to the extracelluar concentration of H2O2.

1.1 Response of intracellular H2O2 is biphasic

When $k_{met} \approx 0$, the $[H_i]/[H_o]$ ratio is bounded between two extremes and increases rapidly when $[H_o]$ passes a certain threshold (Fig. 2, right panel). Interestingly, the lower and upper bound values of the ratio are approximately equal to ratios in Cat- and Ahp- strains, suggesting that the two enzymes play dominant roles in different H2O2 concentration ranges. The lower bound of

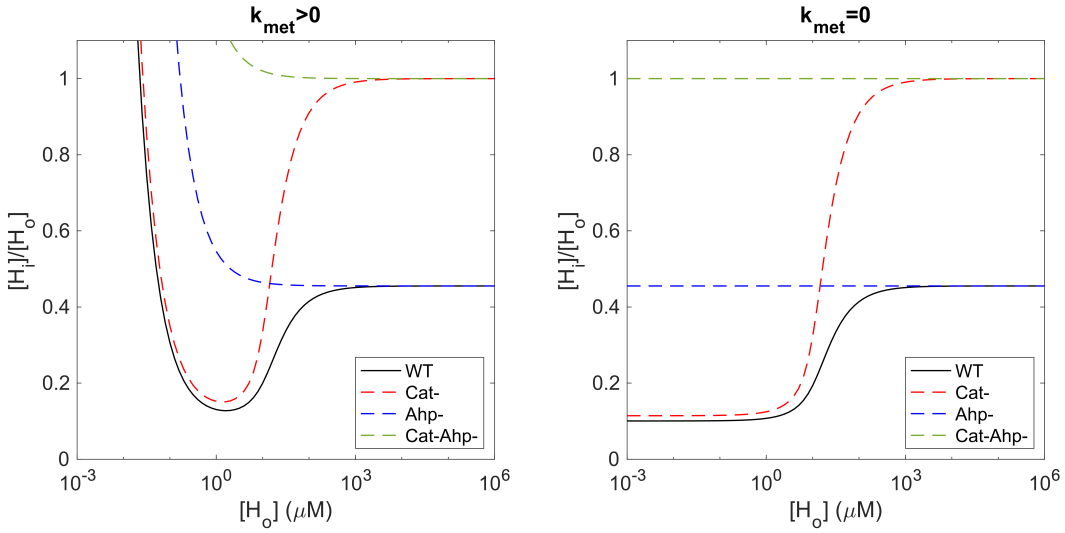

Fig. 2: Relationship between intracellular and extracellular H2O2 concentrations. (Left panel) H2O2 is produced metabolically. (Right panel) H2O2 is NOT produced metabolically.

$[H_i]/[H_o]$ for the wild-type strain can be solved by setting $k_{cat} = 0$

$$[H_i] = \frac{-\left(K_{m,ahp} - [H_o] + \frac{k_{ahp}}{PA}\right) + \sqrt{\left(K_{m,ahp} - [H_o] + \frac{k_{ahp}}{PA}\right)^2 + 4K_{m,ahp}[H_o]}}{2} \tag{4}$$

$$= \frac{K_{m,ahp}}{K_{m,ahp} + \frac{k_{ahp}}{PA}}[H_o] + \mathscr{O}([H_o]^2) \tag{5}$$

If $[H_o]$ is small, we retain the leading term only, giving

$$\left(\frac{[H_i]}{[H_o]}\right)_{lb} = \frac{PA}{PA + \frac{k_{ahp}}{K_{m,ahp}}} \tag{6}$$

Similarly, the upper bound of the ratio can be derived by setting $k_{ahp} = 0$, leading to

$$\left(\frac{[H_i]}{[H_o]}\right)_{ub} = \frac{PA}{PA + k_{cat}} \tag{7}$$

In sum, the H2O2 concentration gradient across membrane is determined by both cell membrane permeability and specific activity of H2O2-scavenging enzymes. The response of intracellular H2O2 is biphasic, which is originated from the differential H2O2 affinity between catalase and Ahp. This biphasic response has been reported in yeast strain *Saccharomyces pombe* [8], where H2O2-triggered hyperoxidation of Prx to thioredoxin-resistant, peroxidase-inactive form is a key to direct available thioredoxin to repair damage. In contrast, bacterial 2-Cys Prx, such as the E. coli peroxiredoxin AhpC, are much less sensitive to hyperoxidation.

1.2 Ultrasensitivity of OxyR oxidation to increasing extracellular H2O2 concentration

OxyR is activated by H2O2 through the oxidation of reactive cysteines. Since OxyR behaves as an autorepressor at the transcriptional level, we assume that the total concentration of OxyR is

a constant ($OxyR_t$). The dynamics of interconversion between oxidized ($[OxyR_{ox}]$) and reduced ($[OxyR_{red}]$) forms of OxyR is given by

$$\frac{d[OxyR_{ox}]}{dt} = \frac{k_{oxyr,ox}[OxyR_{red}][H_i]^{n_{oxyr}}}{K_{m,oxyr}^{n_{oxyr}} + [H_i]^{n_{oxyr}}} - k_{oxyr,red}[OxyR_{ox}] \tag{8}$$

Using $OxyR_t = [OxyR_{ox}] + [OxyR_{red}]$, the fraction of oxidized form of OxyR can be derived as steady state

$$\frac{[OxyR_{ox}]_{ss}}{OxyR_t} = \frac{[H_i]^{n_{oxyr}}}{[H_i]^{n_{oxyr}}\left(1 + \frac{k_{oxyr,red}}{k_{oxyr,ox}}\right) + \frac{k_{oxyr,red}}{k_{oxyr,ox}}K_{m,oxyr}^{n_{oxyr}}} \tag{9}$$

The parameter values can be estimated by fitting experimental data (see Fig. 3)

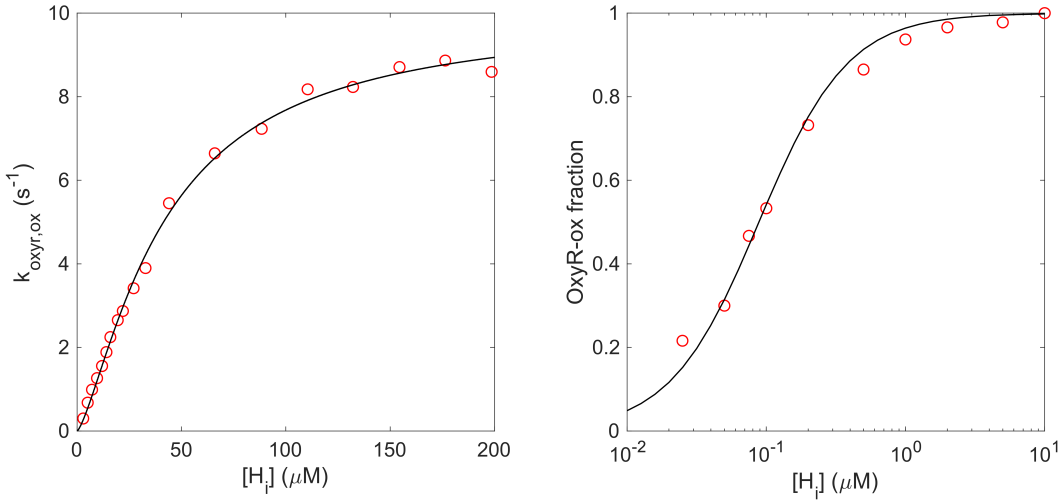

Fig. 3: Fitting OxyR-related parameters to experimental data. Data sources: Left panel [9] and right panel [10]. The best-fit parameter values are $n_{oxyr} = 1.36$, $K_{m,oxyr} = 41.32\ \mu M$, $k_{oxyr,ox} = 9.99\ s^{-1}$, $k_{oxyr,red} = 2.3 \times 10^{-3}\ s^{-1}$. The value of $k_{oxyr,red}$ corresponds to a half life of 5 min, which is consistent with a previous estimate [10].

Although the response of OxyR oxidization to increased intracellular H2O2 is Michaelis-Menten-like, its response to extracellular H2O2 is ultrasensitive (Hill coefficient = 10.7) [11]. The fraction of oxidized OxyR increases sharply over a very narrow range of extracellular H2O2 concentration. This switch-like behavior must come from digital-like change of intracellular H2O2 to extracellular H2O2 concentration. We showed below that $K_{m,ahp}$ is a key parameter to generate such discrete state shift. When $K_{m,ahp}$ is a small parameter, we can expand Eq. 2 using power series of $K_{m,ahp}$

$$[H_i] = \begin{cases} \dfrac{[H_o]PA + k_{met}}{k_{ahp} - [H_o]PA - k_{met}}K_{m,ahp} + \mathcal{O}(K_{m,ahp}^2) & [H_o] < \dfrac{k_{ahp} - k_{met}}{PA} \\ \dfrac{[H_o]PA + k_{met} - k_{ahp}}{PA + k_{cat}} + \dfrac{k_{ahp}}{[H_o]PA + k_{met} - k_{ahp}}K_{m,ahp} + \mathcal{O}(K_{m,ahp}^2) & [H_o] \geq \dfrac{k_{ahp} - k_{met}}{PA} \end{cases}$$

The underlying principle is called zero-order ultrasensitivity [12], which occurs under saturation conditions ($K_{m,ahp} \ll [H_i]$). We showed that decreasing Km_{ahp} indeed makes OxyR response more switch-like (Fig. 4, left panel).

To quantitatively fit the experimental data, we first varied k_{ahp} and $K_{m,ahp}$ at the same time. Although a good fitting can be achieved (Fig. 4, right panel, dashed line), the best-fit value of $K_{m,ahp}$ is below 1 nM, which is unrealistic. Then we tried fitting $K_{m,ahp}$ alone while fixing k_{ahp} (Fig. 4, right panel, solid line). The best-fit $K_{m,ahp}$ is 78.66 nM, which is consistent with previous estimation that the intracellular H2O2 concentration is about 50 nM and an intracellular concentration of about 200 nM is sufficient to drive OxyR into the oxidized form [13].

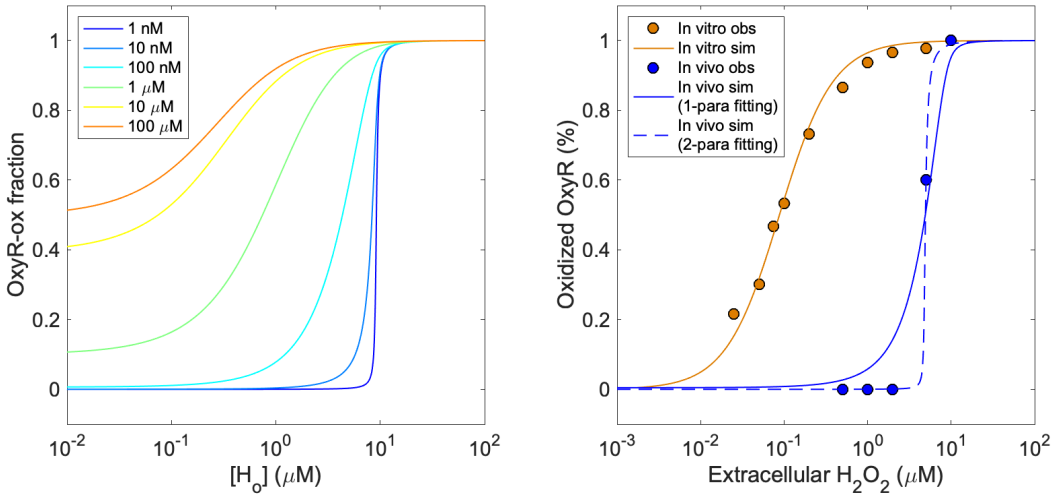

Fig. 4: Single-parameter fitting. (Left panel) OxyR response becomes ultrasensitive with decreased value of $K_{m,ahp}$. (Right panel) Fitting $K_{m,ahp}$ and k_{ahp} to experimental data. For 2-parameter fitting, the best-fit parameter values are $k_{ahp} = 1.12 \times 10^{-18}\ mol/s$ and $K_{m,ahp} = 0.557\ nM$. For single-parameter fitting, the best-fit parameter value is $K_{m,ahp} = 78.66\ nM$.

2 Regulated model (Ahp and KatG expression regulated by OxyR)

We assume that the synthesis rates of Cat and Ahp are proportional to the fraction of the oxidized OxyR

$$\frac{d[H_i]}{dt} = \frac{k_{met} + ([H_o] - [H_i])PA}{V_c} - k_{0,cat}[Cat][H_i] - \frac{k_{0,ahp}[Ahp][H_i]}{K_{m,ahp} + [H_i]} \tag{10}$$

$$\frac{d[H_o]}{dt} = -\frac{([H_o] - [H_i])PA}{V_e} \tag{11}$$

$$\frac{d[Cat]}{dt} = \alpha_{cat} \frac{[H_i]^{n_{oxyr}}}{[H_i]^{n_{oxyr}} \left(1 + \frac{k_{oxyr,red}}{k_{oxyr,ox}}\right) + \frac{k_{oxyr,red}}{k_{oxyr,ox}} K_{m,oxyr}^{n_{oxyr}}} - \lambda[Cat] \tag{12}$$

$$\frac{d[Ahp]}{dt} = \alpha_{ahp} \frac{[H_i]^{n_{oxyr}}}{[H_i]^{n_{oxyr}} \left(1 + \frac{k_{oxyr,red}}{k_{oxyr,ox}}\right) + \frac{k_{oxyr,red}}{k_{oxyr,ox}} K_{m,oxyr}^{n_{oxyr}}} - \lambda[Ahp] \tag{13}$$

where $k_{0,cat}$ and $k_{0,ahp}$ are the H2O2 consumption rates per molecule of respective enzymes, α_{cat} and α_{ahp} are the maximum production rates of respective enzymes, and λ is the specific growth rate. The following parameter values are used: $k_{0,cat} = 4.188 \times 10^6\ (s \cdot M)^{-1}$ [14], $k_{0,ahp} =$

52.4 s^{-1} [15], $\alpha_{cat} = 3.62 \times 10^{-24}\ mol/s$ [16], $\alpha_{ahp} = 1.19 \times 10^{-22}\ mol/s$ [16], $\lambda = 1.93\ h^{-1}$ [16] and $V = 2\ \mu m^3$.

3 Simple cell growth model

1 Derivation of a Minimal Cell Growth Model for *E. coli*

Our kinetic bacterial growth model defines the interplay between the concentrations of precursor $[P]$, ribosomes $[R]$, the global regulator $[X]$, and the specific growth rate of the cell Λ. The dynamics of $[R]$, $[P]$, and $[X]$ are modeled by considering their rates of production minus their rates of consumption and degradation. Namely,

$$\frac{d[P]}{dt} = J_p^{in} - J_p^{out} \tag{14}$$

$$\frac{d[R]}{dt} = J_r^{in} - J_r^{out} \tag{15}$$

$$\frac{d[X]}{dt} = J_x^{in} - J_x^{out} \tag{16}$$

where J_x^{in} is the production rate of molecule x and J_x^{out} is its combined consumption and degradation rate. The specific growth rate is determined with respect to cell volume Ω, which grows exponentially as

$$\Lambda = \frac{1}{\Omega}\frac{d\Omega}{dt} \tag{17}$$

The mathematical representations of these reaction rates are detailed as follows.

1.1 A coarse-grained model of *E. coli* proteome

Recent experimental studies [17, 18] have shown that the proteome of exponentially growing *E. coli* cells can be minimally partitioned into two sectors which each have a distinct role in determining its physiology. Ribosomal and affiliated proteins belong to the R sector, catabolic and anabolic enzymes for nutrient uptake and conversion belong to the E sector. Since the *E. coli* mass density is relatively constant in presence of various perturbations [19, 20] and the majority of biomass is protein [21], the protein density $[O]$ remains unchanged under different growth conditions. That is,

$$[O] = m_r[R] + m_e[E] = \beta \tag{18}$$

1.2 The precursor production, consumption and degradation rates

Under constant or saturating nutrient concentration, the nutrient uptake rate is determined by the availability of metabolic proteins and subject to feedback inhibition by its end products, precursor. That is, when the metabolic intermediates between nutrient and precursor are ignored,

$$J_p^{in} = f_e([E])\frac{[P]}{K_{ip} + [P]} \tag{19}$$

where the function $f_e([E])$ relates the influx of precursor to the concentration of coarse-grained metabolic proteins. For most rate-limiting enzymes that absorb nutrients from environment, the function is linear [22], so

$$f_e([E]) = k_e[E] \tag{20}$$

where k_e is a linear coefficient that represents the nutrient quality.

In this framework, precursors are utilized solely for protein synthesis and not for other metabolic reactions. Since each active ribosome is able to initiate translation, the consumption rate of precursor (J_p^{con}) in protein synthesis is modelled using a Michaelis-Menten equation

$$J_{con}^{p} = \frac{k_r[R][P]}{K_{mp} + [P]} \tag{21}$$

We assume precursors are only diluted via volume expansion, so

$$J_p^{deg} = \Lambda[P] \tag{22}$$

is the degradation rate. The total precursor outflux rate is the sum of the reaction rates from both utilization via protein synthesis and dilution via volume expansion, that is,

$$J_p^{out} = J_p^{con} + J_p^{deg} \tag{23}$$

1.3 The ribosome synthesis and degradation rates

It is generally believed that the synthesis of ribosomal RNAs is the limiting step in ribosome production due to excessive ribosomal proteins than ribosomal RNAs [23]. On the other hand, ribosome production is also limited by the synthesis of ribosomal proteins in terms of reaction dynamics because protein synthesis takes much longer time as compared to RNA synthesis. Considering the dynamic nature of our minimal model, we assume the latter, meaning that the ribosome production rate J_r^{in} is determined by the fraction of total translational capacity allocated for producing R sector proteins. Additionally, because ppGpp inhibits transcription initiation of ribosomal proteins both *in vitro* and *in vivo* [24], a function α_r that describes the degree of inhibition is included. The ribosome production rate is then

$$J_r^{in} = \frac{J_p^{con}\alpha_r}{m_r} \tag{24}$$

The regulation of ribosome by the global regulatory X is written as a Michaelis-Menten function

$$\alpha_r = \frac{K_{ix}}{[X] + K_{ix}} \tag{25}$$

where K_{ix} is the regulator concentration at which half of ribosome synthesis is halted.

Ribosomes are very stable in fast growth but are degraded in starvation, entry into stationary phase, and slow growth [25, 26]. For simplicity, we assume ribosomes are not degraded but decay due to dilution effect

$$J_r^{out} = \Lambda[R] \tag{26}$$

1.4 The synthesis and degradation rates of global regulator

We assume the synthesis rate of global regulator X is inversely regulated by the precursor concentration

$$J_x^{in} = k_x \frac{K_{mp}}{K_{mp} + [P]} \tag{27}$$

where k_x is the maximal synthesis rate.

The turnover rate of global regulator is generally much faster than the decay rate due to dilution. Therefore, we assume first-order active degradation and ignore the dilution effect

$$J_x^{out} = d_x[X] \tag{28}$$

where d_x is the first order degradation rate constant.

1.5 The specific growth rate

Using the previous assumption that the intracellular protein density is constant, the specific growth rate Λ is determined by the rate of protein production

$$\Lambda = \frac{1}{\Omega}\frac{d\Omega}{dt} = \frac{1}{\beta}\left(\frac{1}{\Omega}\frac{dO}{dt}\right) = \frac{J_p^{con}}{\beta} \tag{29}$$

1.6 Summary

The entire model equations are summarized below

$$\frac{d[(H_2O_2)_{in}]}{dt} = \underbrace{k_e[E]}_{\substack{\text{maximum precursor}\\ \text{synthesis rate}}} \underbrace{\frac{K_{ip}}{K_{ip}+[P]}}_{\substack{\text{feedback}\\ \text{inhibition}}} - \underbrace{\frac{k_r[R][P]}{K_{mp}+[P]}}_{\substack{\text{precursor}\\ \text{consumption rate}}} - \underbrace{\Lambda[P]}_{\substack{\text{precursor}\\ \text{dilution rate}}} \tag{30}$$

$$\frac{d[P]}{dt} = \underbrace{k_e[E]}_{\substack{\text{maximum precursor}\\ \text{synthesis rate}}} \underbrace{\frac{K_{ip}}{K_{ip}+[P]}}_{\substack{\text{feedback}\\ \text{inhibition}}} - \underbrace{\frac{k_r[R][P]}{K_{mp}+[P]}}_{\substack{\text{precursor}\\ \text{consumption rate}}} - \underbrace{\Lambda[P]}_{\substack{\text{precursor}\\ \text{dilution rate}}} \tag{31}$$

$$\frac{d[R]}{dt} = \underbrace{\frac{k_r[R][P]}{m_r(K_{mp}+[P])}\frac{K_{ix}}{K_{ix}+[X]}}_{\substack{\text{ribosome}\\ \text{synthesis rate}}} - \underbrace{\Lambda[R]}_{\substack{\text{ribosome}\\ \text{dilution rate}}} \tag{32}$$

$$\frac{d[X]}{dt} = \underbrace{k_x\frac{K_{mp}}{K_{mp}+[P]}}_{\substack{\text{regulator}\\ \text{synthesis rate}}} - \underbrace{d_x[X]}_{\substack{\text{regulator}\\ \text{degradation rate}}} \tag{33}$$

$$\Lambda = \underbrace{\frac{k_r[R][P]}{\beta(K_{mp}+[P])}}_{\text{specific growth rate}} \tag{34}$$

$$[E] = \underbrace{\frac{\beta - m_r[R]}{m_e}}_{\substack{\text{metabolic protein}\\ \text{concentration}}} \tag{35}$$

2 Nondimensionalization

The following transformations are made:
$p = [P]/\beta$, $r = m_r[R]/\beta$, $x = [X]/\beta$, $\tau = k_r t/m_r$, $\lambda = m_r\Lambda/k_r$, $k'_e = m_r k_e/(k_r m_e)$, $k'_x = (k_x m_r)/(k_r\beta)$, $d'_x = d_x m_r/k_r$, $K'_{mp} = K_{mp}/\beta$, $K'_{ix} = K_{ix}/\beta$, $K'_{ip} = K_{ip}/\beta$.

$$\frac{dp}{d\tau} = k'_e(1-r)\frac{K'_{ip}}{K'_{ip}+p} - \lambda(1+p) \tag{36}$$

$$\frac{dr}{d\tau} = \lambda\left(\frac{K'_{ix}}{K'_{ix}+x} - r\right) \tag{37}$$

$$\frac{dx}{d\tau} = k'_x\frac{K'_{mp}}{K'_{mp}+p} - d'_x x \tag{38}$$

$$\lambda = \frac{rp}{K'_{mp}+p} \tag{39}$$

3 Parameters

Symbol	Description	Value	Unit	Formula	Source
m_r	# of precursor in a ribosome	11738		7336×1.6	[27]
m_e	# of precursor in a metabolic protein	325			[28]
k_r	maximum rate of peptide elongation	7.56×10^4	1/hr	$21\,1/\mathrm{s} \times 3600\,\mathrm{s/hr}$	[29]
k_x	maximum rate of ppGpp synthesis	3.6×10^3	1/hr	$1\,1/\mathrm{s} \times 3600\,\mathrm{s/hr}$	[29]
d_x	first-order rate constant of ppGpp degradation	1.26×10^2	1/hr	$0.035\,1/\mathrm{s} \times 3600\,\mathrm{s/hr}$	[29]
K_{mp}	dissociation constant for amino acid	2.00×10^1	μM		[29]
K_{ix}	dissociation constant for ppGpp	6.00×10^1	μM		
β	total peptide concentration	3.00×10^6	μM		[29]
K_{ip}	precursor feedback inhibition constant	1.00×10^4	μM		

Table 1: Model parameters used in the model.

4 Steady state solution

Let $p \ll K'_{ip}$ so that $K'_{ip}/(K'_{ip}+p) \approx 1$. Combining Eq. 36 and Eq. 39 gives

$$\lambda = \frac{k'_e}{1+p+k'_e\dfrac{K'_{mp}+p}{p}} \tag{40}$$

Similarly, combining Eq. 37 and Eq. 38 gives

$$\lambda = \frac{K'_{ix}p}{K'_{ix}(K'_{mp}+p)+\dfrac{k'_x K'_{mp}}{d'_x}} \tag{41}$$

Combining the two equations above gives $p^2+p-\frac{k'_e k'_x K'_{mp}}{K'_{ix}d'_x}=0$, whose solution is given by

$$p = \frac{-1+\sqrt{1+\dfrac{4k'_e k'_x K'_{mp}}{K'_{ix}d'_x}}}{2} \tag{42}$$

Accordingly, the growth rate λ is rewritten as

$$\lambda = \frac{k'_e}{k'_e+\dfrac{1}{2}\left(1+\sqrt{1+\dfrac{4k'_e k'_x K'_{mp}}{K'_{ix}d'_x}}\right)\left(1+\dfrac{K'_{ix}d'_x}{k'_x}\right)} \tag{43}$$

4 Cell growth model with fermentation and ATP limitation

1 Derivation of a cell growth model for *E.coli* with fermentation and ATP limitation

Two more variables are introduced to account for the fermentation and overflow. $[A_{ex}]$ represents the fermentation product inside the cell. We also assumes that the growth rate can be carbon

limited/precursor limited or ATP limited. So the growth rate is the minimum of carbon limited growth rate and ATP limited growth rate. Further, the precursor consumption rate is also assumed to be dependent on the ATP flux. The model equations with fermentation and ATP limitation are as follows:

$$\frac{d[P]}{dt} = \underbrace{\frac{k_e[E][S_{ex}]}{K_{ms}+[S_{ex}]}}_{\text{maximum precursor synthesis rate}} \underbrace{\frac{K_{ip}}{K_{ip}+[P]}}_{\text{feedback inhibition}} - \underbrace{\beta\Lambda}_{\text{precursor consumption rate}} - \underbrace{\Lambda[P]}_{\text{precursor dilution rate}} - \underbrace{\frac{v_a[P]\left(1-\frac{1}{K_{ca}}\frac{[A_{ex}]}{[P]}\right)}{K_{ma}+[P]\left(1+k_{ra}\frac{1}{K_{ca}}\frac{[A_{ex}]}{[P]}\right)}}_{\text{reversible fermentation rate with thermodynamic constrait}} + \underbrace{\frac{k_u[E][A_{ex}]}{K_{mu}+[A_{ex}]}}_{\text{fermentation product uptake rate}} - \underbrace{\frac{k_o[E][P]}{K_{mo}+[P]}}_{\text{rate of TCA cycle}}$$

$$\frac{d[R]}{dt} = \underbrace{\frac{\beta\Lambda}{m_r}\frac{K_{ix}}{K_{ix}+[X]}}_{\text{ribosome synthesis rate}} - \underbrace{\Lambda[R]}_{\text{ribosome dilution rate}}$$

$$\frac{d[X]}{dt} = \underbrace{k_x\frac{K_{mp}}{K_{mp}+[P]}}_{\text{regulator synthesis rate}} - \underbrace{d_x[X]}_{\text{regulator degradation rate}}$$

$$\Lambda_b = \underbrace{\frac{k_r[R][P]}{\beta(K_{mp}+[P])}}_{\text{carbon limited growth rate}}$$

$$\Lambda_e = \underbrace{\sigma\left(n_p\frac{k_e[E][S_{ex}]}{K_{ms}+[S_{ex}]}\frac{K_{ip}}{K_{ip}+[P]} + n_a\left(\frac{v_a[P]\left(1-\frac{1}{K_{ca}}\frac{[A_{ex}]}{[P]}\right)}{K_{ma}+[P]\left(1+k_{ra}\frac{1}{K_{ca}}\frac{[A_{ex}]}{[P]}\right)} - \frac{k_u[E][A_{ex}]}{K_{mu}+[A_{ex}]}\right) + n_o\frac{k_o[E][P]}{K_{mo}+[P]}\right)}_{\text{ATP limited growth rate}}$$

$$\Lambda = \min\{\Lambda_b, \Lambda_e\}$$

$$[E] = \underbrace{\frac{\beta - m_r[R]}{m_e}}_{\text{metabolic protein concentration}}$$

2 Nondimensionalization

The transformations are as follows: $p=[P]/\beta$, $r=m_r[R]/\beta$, $x=[X]/\beta$, $\tau=k_r t/m_r$, $\lambda=m_r\Lambda/k_r$, $k'_e=m_r k_e/(k_r m_e)$, $k'_x=(k_x m_r)/(k_r\beta)$, $d'_x=d_x m_r/k_r$, $K'_{mp}=K_{mp}/\beta$, $K'_{ix}=K_{ix}/\beta$, $K'_{ip}=K_{ip}/\beta$, $v'_a=m_r v_a/(k_r\beta)$, $K'_{ma}=K_{ma}/\beta$, $k'_u=m_r k_u/(k_r m_e)$, $K'_{mu}=K_{mu}/\beta$, $n'_p=\sigma\beta n_p$, $n'_a=\sigma\beta n_a$.

$$\frac{dp}{d\tau} = k'_e(1-r)\frac{K'_{ip}}{K'_{ip}+p} - \lambda - \lambda p - \frac{v'_a p\left(1-\frac{1}{K_{ca}}\frac{A_{ex}}{p}\right)}{K'_{ma}+p\left(1+\frac{k_{ra}}{K_{ca}}\frac{A_{ex}}{p}\right)} + \frac{k'_u(1-r)A_{ex}}{K'_{mu}+A_{ex}} \tag{44}$$

$$\frac{dr}{d\tau} = \lambda\frac{K'_{ix}}{K'_{ix}+x} - \lambda r \tag{45}$$

$$\frac{dx}{d\tau} = k'_x\frac{K'_{mp}}{K'_{mp}+p} - d'_x x \tag{46}$$

$$\frac{dA_{ex}}{d\tau} = \frac{v'_a p\left(1-\frac{1}{K_{ca}}\frac{A_{ex}}{p}\right)}{K'_{ma}+p\left(1+\frac{k_{ra}}{K_{ca}}\frac{A_{ex}}{p}\right)} - \frac{k'_u(1-r)A_{ex}}{K'_{mu}+A_{ex}} - \lambda A_{ex} \tag{47}$$

$$\lambda_b = \frac{rp}{K'_{mp}+p} \tag{48}$$

$$\lambda_e = n'_p k'_e (1-r)\frac{K'_{ip}}{K'_{ip}+p} + n'_a \frac{v'_a p\left(1-\frac{1}{K_{ca}}\frac{A_{ex}}{p}\right)}{K'_{ma}+p\left(1+\frac{k_{ra}}{K_{ca}}\frac{A_{ex}}{p}\right)} \quad (49)$$

$$\lambda = \min\{\lambda_b, \lambda_e\} \quad (50)$$

3 Parameters

Symbol	Description	Value	Unit	Source
k_e	maximum rate of glucose uptake	8.67×10^3	h^{-1}	estimated from Enjalbert *et al.*, 2017
K_{ms}	Michaelis constant for glucose uptake	6.67	μM	Jahan *et al.*, 2016
m_r	# of aa. (precursor) in a ribosome	11738 (7336×1.6)		Bremer and Dennis, 2008
m_e	# of aa. (precursor) in a metabolic protein	325		Maitra *et al.*, 2015
k_r	maximum rate of peptide elongation	7.56×10^4	h^{-1}	Marr, 1991
k_x	maximum rate of ppGpp (regulator) synthesis	3.6×10^3	h^{-1}	Marr, 1991
d_x	first-order rate constant of ppGpp (regulator) degradation	1.26×10^2	h^{-1}	Marr, 1991
K_{mp}	dissociation constant for aa. (precursor)	2.00×10^1	μM	Marr, 1991
K_{ix}	dissociation constant for ppGpp (regulator)	6.00×10^1	μM	assumed
β	total aa. (precursor) concentration	3.00×10^6	μM	Marr, 1991
K_{ip}	aa. (precursor) feedback inhibition constant	1.00×10^4	μM	assumed
v_a	maximum rate of acetate (fermentation product) production	1.62×10^8	$\mu M/h$	Jahan *et al.*, 2016
K_{ma}	Michaelis constant for acetate (fermentation product) production	1.60×10^2	μM	Jahan *et al.*, 2016
K_{ca}	equilibrium constant	4.88×10^1		estimated from Enjalbert *et al.*, 2017
k_{ra}	ratio between maximal forward and reverse rate	1.00	μM	assumed
k_u	maximum rate of acetate (fermentation production) reuptake	9.80×10^3	h^{-1}	estimated from Enjalbert *et al.*, 2017
K_{mu}	Michaelis constant for acetate (fermentation product) reuptake	1.67×10^1	μM	Jahan *et al.*, 2016
$P{:}O$	ATP produced per NADH or $FADH_2$	2.02		estimated from Enjalbert *et al.*, 2017
n_p	ATP yield of glycolysis	10.08		$2+4(P{:}O)$
n_a	ATP yield of fermentation	1		$1+0(P{:}O)$
n_r	ATP yield of TCA	9.08		$1+4(P{:}O)$
σ	growth rate per ATP production flux	8.87×10^{-9}	μM^{-1}	Jahan *et al.*, 2016

Table 2: Model parameters used in the model.

5 Cell growth model with fermentation and overflow

1 Derivation of a cell growth model for *E.coli* with fermentation and overflow

Two more variables are introduced to account for the fermentation and overflow. $[A_{ex}]$ represents the fermentation product inside the cell. $[A_{ex}]$ is the same fermentaion production outside the cell. The N represents the cell number. The model equations with fermentation and overflow are as follows:

$$\frac{dN}{dt} = \underbrace{\Lambda N}_{\text{growth rate}} - \underbrace{\delta N}_{\text{dilution rate}} \quad (51)$$

$$\frac{d[P]}{dt} = \underbrace{k_e[E]}_{\substack{\text{maximum precursor}\\ \text{synthesis rate}}} \underbrace{\frac{K_{ip}}{K_{ip}+[P]}}_{\substack{\text{feedback}\\ \text{inhibition}}} - \underbrace{\beta\Lambda}_{\substack{\text{precursor}\\ \text{consumption rate}}} - \underbrace{\Lambda[P]}_{\substack{\text{precursor}\\ \text{dilution rate}}}$$

$$- \underbrace{\frac{v_a[P](1-\frac{1}{K_{ca}}\frac{[A_{in}]}{[P]})}{K_{mp}+[P](1+k_{ra}\frac{1}{K_{ca}}\frac{[A_{in}]}{[P]})}}_{\substack{\text{reversible fermentation rate}\\ \text{with thermodynamic constrait}}} + \underbrace{\frac{k_u[E][A_{in}]}{K_{mu}+[A_{in}]}}_{\substack{\text{fermentation product}\\ \text{uptake rate}}} \tag{52}$$

$$\frac{d[R]}{dt} = \underbrace{\frac{\beta\Lambda}{m_r}\frac{K_{ix}}{K_{ix}+[X]}}_{\substack{\text{ribosome}\\ \text{synthesis rate}}} - \underbrace{\Lambda[R]}_{\substack{\text{ribosome}\\ \text{dilution rate}}} \tag{53}$$

$$\frac{d[X]}{dt} = \underbrace{k_x\frac{K_{mp}}{K_{mp}+[P]}}_{\substack{\text{regulator}\\ \text{synthesis rate}}} - \underbrace{d_x[X]}_{\substack{\text{regulator}\\ \text{degradation rate}}} \tag{54}$$

$$\frac{d[A_{in}]}{dt} = \underbrace{\frac{v_a[P](1-\frac{1}{K_{ca}}\frac{[A_{in}]}{[P]})}{K_{mp}+[P](1+k_{ra}\frac{1}{K_{ca}}\frac{[A_{in}]}{[P]})}}_{\substack{\text{reversible fermentation rate}\\ \text{with thermodynamic constrait}}} - \underbrace{\frac{k_u[E][A_{in}]}{K_{mu}+[A_{in}]}}_{\substack{\text{fermentation product}\\ \text{uptake rate}}} + \underbrace{D([A_{ex}]-[A_{in}])}_{\substack{\text{diffusion of}\\ \text{fermentation product}}} - \underbrace{\Lambda[A_{in}]}_{\substack{\text{dilution rate}}} \tag{55}$$

$$\frac{d[A_{ex}]}{dt} = \underbrace{-D([A_{ex}]-[A_{in}])(\frac{V_cN}{V_m})}_{\substack{\text{diffusion of}\\ \text{fermentation product}}} - \underbrace{\delta[A_{ex}]}_{\substack{\text{dilution of extracellular}\\ \text{fermentation product}}} \tag{56}$$

$$\Lambda_b = \underbrace{\frac{k_r[R][P]}{\beta(K_{mp}+[P])}}_{\substack{\text{carbon limited}\\ \text{growth rate}}} \tag{57}$$

$$\Lambda_e = \underbrace{n_pk_e[E]\frac{K_{ip}}{K_{ip}+[P]} + n_a\frac{v_a[P](1-\frac{1}{K_{ca}}\frac{[A_{ex}]}{[P]})}{K_{mp}+[P](1+k_{ra}\frac{1}{K_{ca}}\frac{[A_{ex}]}{[P]})}}_{\substack{\text{ATP limited}\\ \text{growth rate}}} \tag{58}$$

$$\Lambda = min\{\Lambda_b, \Lambda_e\} \tag{59}$$

$$[E] = \underbrace{\frac{\beta - m_r[R]}{m_e}}_{\substack{\text{metabolic protein}\\ \text{concentration}}} \tag{60}$$

2 Nondimensionlization

The transformations are as follows: $p=[P]/\beta$, $r=m_r[R]/\beta$, $x=[X]/\beta$, $a_{in}=A_{in}/\beta$, $a_{ex}=A_{ex}/\beta$, $\tau=k_rt/m_r$, $\lambda=m_r\Lambda/k_r$, $k'_e=m_rk_e/(k_rm_e)$, $k'_x=(k_xm_r)/(k_r\beta)$, $d'_x=d_xm_r/k_r$, $K'_{mp}=K_{mp}/\beta$, $K'_{ix}=K_{ix}/\beta$, $K'_{ip}=K_{ip}/\beta$, $v'_a=m_rv_a/(k_r\beta)$, $K'_{ma}=K_{ma}/\beta$, $k'_u=m_rk_u/(k_rm_e)$, $K'_{mu}=K_{mu}/\beta$, $n'_p=\sigma\beta n_p$, $n'_a=\sigma\beta n_a$, $\delta'=m_r\delta/k_r$, $D'=m_rD/k_r$.

$$\frac{dN}{d\tau} = \lambda N - \delta' N \tag{61}$$

$$\frac{dp}{d\tau} = k'_e(1-r)\frac{K'_{ip}}{K'_{ip}+p} - \lambda - \lambda p - \frac{v'_ap\left(1-\frac{1}{K_{ca}}\frac{a_{in}}{p}\right)}{K'_{ma}+p\left(1+\frac{k_{ra}}{K_{ca}}\frac{a_{in}}{p}\right)} + \frac{k'_u(1-r)A_{ex}}{K'_{mu}+a_{in}} \tag{62}$$

$$\frac{dr}{d\tau} = \lambda \frac{K'_{ix}}{K'_{ix}+x} - \lambda r \tag{63}$$

$$\frac{dx}{d\tau} = k'_x \frac{K'_{mp}}{K'_{mp}+p} - d'_x x \tag{64}$$

$$\frac{da_{in}}{d\tau} = \frac{v'_a p\left(1-\frac{1}{K_{ca}}\frac{a_{in}}{p}\right)}{K'_{ma}+p\left(1+\frac{k_{ra}}{K_{ca}}\frac{a_{in}}{p}\right)} - \frac{k'_u(1-r)a_{in}}{K'_{mu}+a_{in}} + D'(a_{ex}-a_{in}) - \lambda a_{in} \tag{65}$$

$$\frac{da_{ex}}{d\tau} = -D'(a_{ex}-a_{in})\frac{V_c N}{V_m} - \delta' a_{ex} \tag{66}$$

$$\lambda_b = \frac{rp}{K'_{mp}+p} \tag{67}$$

$$\lambda_e = n'_p k'_e (1-r)\frac{K'_{ip}}{K'_{ip}+p} + n'_a \frac{v'_a p\left(1-\frac{1}{K_{ca}}\frac{A_{ex}}{p}\right)}{K'_{ma}+p\left(1+\frac{k_{ra}}{K_{ca}}\frac{A_{ex}}{p}\right)} \tag{68}$$

$$\lambda = \min\{\lambda_b, \lambda_e\} \tag{69}$$

3 Parameters

Symbol	Description	Value	Unit	Formula	Source
m_r	# of precursor in a ribosome	11738		7336×1.6	[27]
m_e	# of precursor in a metabolic protein	325			[28]
k_r	maximum rate of peptide elongation	7.56×10^4	1/hr	$21\,{}^1/_{\mathrm{s}} \times 3600\,{}^{\mathrm{s}}/_{\mathrm{hr}}$	[29]
k_x	maximum rate of ppGpp synthesis	3.6×10^3	1/hr	$1\,{}^1/_{\mathrm{s}} \times 3600\,{}^{\mathrm{s}}/_{\mathrm{hr}}$	[29]
d_x	first-order rate constant of ppGpp degradation	1.26×10^2	1/hr	$0.035\,{}^1/_{\mathrm{s}} \times 3600\,{}^{\mathrm{s}}/_{\mathrm{hr}}$	[29]
K_{mp}	dissociation constant for amino acid	2.00×10^1	μM		[29]
K_{ix}	dissociation constant for ppGpp	6.00×10^1	μM		
β	total peptide concentration	3.00×10^6	μM		[29]
K_{ip}	precursor feedback inhibition constant	1.00×10^4	μM		
v_a	constant	1.00×10^4	μM		
K_{ma}	constant	1.00×10^4	μM		
k_u	constant	1.00×10^4	μM		
$K_m u$	constant	1.00×10^4	μM		
n_p	constant	1.00×10^4	μM		
n_a	constant	1.00×10^4	μM		
σ	constant	1.00×10^4	μM		
K_{ca}	constant	1.00×10^4	μM		
k_{ra}	constant	1.00×10^4	μM		

Table 3: Model parameters used in the model.

6 Cell growth model with fermentation and overflow in space

1 Derivation of a cell growth model for *E.coli* with fermentation and overflow in space

Two more variables are introduced to account for the fermentation and overflow. $[A_{ex}]$ represents the fermentation product inside the cell. $[A_{ex}]$ is the same fermentaion production outside the cell. The N represents the cell number. The model equations with fermentation and overflow are as follows:

$$\frac{\partial N}{\partial t} = \underbrace{D_N \frac{\partial^2 N}{\partial x^2}}_{\text{diffusion of bacteria}} + \underbrace{v\frac{\partial N}{\partial x}}_{\text{flow rate}} + \underbrace{\Lambda N}_{\text{growth rate}} - \underbrace{\delta N}_{\text{dilution rate}} \tag{70}$$

$$\frac{\partial [P]}{\partial t} = \underbrace{\frac{k_e[E][S]}{K_{ms}+[S]}}_{\substack{\text{maximum precursor}\\ \text{synthesis rate}}} \underbrace{\frac{K_{ip}}{K_{ip}+[P]}}_{\substack{\text{feedback}\\ \text{inhibition}}} - \underbrace{\beta\Lambda}_{\substack{\text{precursor}\\ \text{consumption rate}}} - \underbrace{\Lambda[P]}_{\substack{\text{precursor}\\ \text{dilution rate}}}$$

$$- \underbrace{\frac{v_a[P](1-\frac{1}{K_{ca}}\frac{[A_{in}]}{[P]})}{K_{mp}+[P](1+k_{ra}\frac{1}{K_{ca}}\frac{[A_{in}]}{[P]})}}_{\substack{\text{reversible fermentation rate}\\ \text{with thermodynamic constrait}}} + \underbrace{\frac{k_u[E][A_{in}]}{K_{mu}+[A_{in}]}}_{\substack{\text{fermentation product}\\ \text{uptake rate}}} \tag{71}$$

$$\frac{\partial [R]}{\partial t} = \underbrace{\frac{\beta\Lambda}{m_r}\frac{K_{ix}}{K_{ix}+[X]}}_{\substack{\text{ribosome}\\ \text{synthesis rate}}} - \underbrace{\Lambda[R]}_{\substack{\text{ribosome}\\ \text{dilution rate}}} \tag{72}$$

$$\frac{\partial [X]}{\partial t} = \underbrace{k_x\frac{K_{mp}}{K_{mp}+[P]}}_{\substack{\text{regulator}\\ \text{synthesis rate}}} - \underbrace{d_x[X]}_{\substack{\text{regulator}\\ \text{degradation rate}}} \tag{73}$$

$$\frac{\partial [A_{in}]}{\partial t} = \underbrace{\frac{v_a[P](1-\frac{1}{K_{ca}}\frac{[A_{in}]}{[P]})}{K_{mp}+[P](1+k_{ra}\frac{1}{K_{ca}}\frac{[A_{in}]}{[P]})}}_{\substack{\text{reversible fermentation rate}\\ \text{with thermodynamic constrait}}} - \underbrace{\frac{k_u[E][A_{in}]}{K_{mu}+[A_{in}]}}_{\substack{\text{fermentation product}\\ \text{uptake rate}}} + \underbrace{D([A_{ex}]-[A_{in}])}_{\substack{\text{diffusion of}\\ \text{fermentation product}}} - \underbrace{\Lambda[A_{in}]}_{\substack{\text{dilution rate}}} \tag{74}$$

$$\frac{\partial [A_{ex}]}{\partial t} = \underbrace{D_A\frac{\partial^2[A_{ex}]}{\partial x^2}}_{\substack{\text{diffusion of}\\ \text{fermentation product}}} + \underbrace{v\frac{\partial [A_{ex}]}{\partial x}}_{\text{flow rate}} \underbrace{-D([A_{ex}]-[A_{in}])(\frac{V_c N}{V_m})}_{\substack{\text{diffusion of}\\ \text{fermentation product}}} - \underbrace{\delta[A_{ex}]}_{\substack{\text{dilution of extracellular}\\ \text{fermentation product}}} \tag{75}$$

$$\frac{\partial [S]}{\partial t} = \underbrace{D_S\frac{\partial^2[S]}{\partial x^2}}_{\substack{\text{diffusion of}\\ \text{fermentation product}}} + \underbrace{v\frac{\partial [S]}{\partial x}}_{\text{flow rate}} - \underbrace{\frac{k_e[E][S]}{K_{ms}+[S]}}_{\substack{\text{maximum substrate}\\ \text{uptake rate}}} \underbrace{\frac{K_{ip}}{K_{ip}+[P]}}_{\substack{\text{feedback}\\ \text{inhibition}}} \tag{76}$$

$$\Lambda_b = \underbrace{\frac{k_r[R][P]}{\beta(K_{mp}+[P])}}_{\substack{\text{carbon limited}\\ \text{growth rate}}} \tag{77}$$

$$\Lambda_e = \underbrace{n_p \frac{k_e[E][S]}{K_{ms}+[S]} \frac{K_{ip}}{K_{ip}+[P]} + n_a \frac{v_a[P](1-\frac{1}{K_{ca}}\frac{[A_{ex}]}{[P]})}{K_{mp}+[P](1+k_{ra}\frac{1}{K_{ca}}\frac{[A_{ex}]}{[P]})}}_{\text{ATP limited growth rate}} \tag{78}$$

$$\Lambda = min\{\Lambda_b, \Lambda_e\} \tag{79}$$

$$[E] = \underbrace{\frac{\beta - m_r[R]}{m_e}}_{\text{metabolic protein concentration}} \tag{80}$$

2 Nondimensionlization

The transformations are as follows: $p = [P]/\beta$, $r = m_r[R]/\beta$, $x = [X]/\beta$, $a_{in} = A_{in}/\beta$, $a_{ex} = A_{ex}/\beta$, $\tau = k_r t/m_r$, $\lambda = m_r\Lambda/k_r$, $k'_e = m_r k_e/(k_r m_e)$, $k'_x = (k_x m_r)/(k_r\beta)$, $d'_x = d_x m_r/k_r$, $K'_{mp} = K_{mp}/\beta$, $K'_{ix} = K_{ix}/\beta$, $K'_{ip} = K_{ip}/\beta$, $v'_a = m_r v_a/(k_r\beta)$, $K'_{ma} = K_{ma}/\beta$, $k'_u = m_r k_u/(k_r m_e)$, $K'_{mu} = K_{mu}/\beta$, $n'_p = \sigma\beta n_p$, $n'_a = \sigma\beta n_a$, $\delta' = m_r\delta/k_r$, $D' = m_r D/k_r$.

$$\frac{dN}{d\tau} = \lambda N - \delta' N \tag{81}$$

$$\frac{dp}{d\tau} = k'_e(1-r)\frac{K'_{ip}}{K'_{ip}+p} - \lambda - \lambda p - \frac{v'_a p\left(1-\frac{1}{K_{ca}}\frac{a_{in}}{p}\right)}{K'_{ma}+p\left(1+\frac{k_{ra}}{K_{ca}}\frac{a_{in}}{p}\right)} + \frac{k'_u(1-r)A_{ex}}{K'_{mu}+a_{in}} \tag{82}$$

$$\frac{dr}{d\tau} = \lambda\frac{K'_{ix}}{K'_{ix}+x} - \lambda r \tag{83}$$

$$\frac{dx}{d\tau} = k'_x\frac{K'_{mp}}{K'_{mp}+p} - d'_x x \tag{84}$$

$$\frac{da_{in}}{d\tau} = \frac{v'_a p\left(1-\frac{1}{K_{ca}}\frac{a_{in}}{p}\right)}{K'_{ma}+p\left(1+\frac{k_{ra}}{K_{ca}}\frac{a_{in}}{p}\right)} - \frac{k'_u(1-r)a_{in}}{K'_{mu}+a_{in}} + D'(a_{ex}-a_{in}) - \lambda a_{in} \tag{85}$$

$$\frac{da_{ex}}{d\tau} = -D'(a_{ex}-a_{in})\frac{V_c N}{V_m} - \delta' a_{ex} \tag{86}$$

$$\lambda_b = \frac{rp}{K'_{mp}+p} \tag{87}$$

$$\lambda_e = n'_p k'_e(1-r)\frac{K'_{ip}}{K'_{ip}+p} + n'_a\frac{v'_a p\left(1-\frac{1}{K_{ca}}\frac{A_{ex}}{p}\right)}{K'_{ma}+p\left(1+\frac{k_{ra}}{K_{ca}}\frac{A_{ex}}{p}\right)} \tag{88}$$

$$\lambda = \min\{\lambda_b, \lambda_e\} \tag{89}$$

Symbol	Description	Value	Unit	Formula	Source
m_r	# of precursor in a ribosome	11738		7336×1.6	[27]
m_e	# of precursor in a metabolic protein	325			[28]
k_r	maximum rate of peptide elongation	7.56×10^4	1/hr	$21\,1/\mathrm{s} \times 3600\,\mathrm{s}/\mathrm{hr}$	[29]
k_x	maximum rate of ppGpp synthesis	3.6×10^3	1/hr	$1\,1/\mathrm{s} \times 3600\,\mathrm{s}/\mathrm{hr}$	[29]
d_x	first-order rate constant of ppGpp degradation	1.26×10^2	1/hr	$0.035\,1/\mathrm{s} \times 3600\,\mathrm{s}/\mathrm{hr}$	[29]
K_{mp}	dissociation constant for amino acid	2.00×10^1	μM		[29]
K_{ix}	dissociation constant for ppGpp	6.00×10^1	μM		
β	total peptide concentration	3.00×10^6	μM		[29]
K_{ip}	precursor feedback inhibition constant	1.00×10^4	μM		
v_a	constant	1.00×10^4	μM		
K_{ma}	constant	1.00×10^4	μM		
k_u	constant	1.00×10^4	μM		
$K_m u$	constant	1.00×10^4	μM		
n_p	constant	1.00×10^4	μM		
n_a	constant	1.00×10^4	μM		
σ	constant	1.00×10^4	μM		
K_{ca}	constant	1.00×10^4	μM		
k_{ra}	constant	1.00×10^4	μM		

Table 4: Model parameters used in the model.

3 Parameters

7 Multiple strains growth model with fermentation and overflow

1 Derivation of multiple strains growth model for *E.coli* with fermentation and overflow

Two strains of bacteria are introduced into the system, labeled by i (=1,2...) The model equations with fermentation and overflow are as follows:

$$\frac{dN_i}{dt} = \underbrace{\Lambda N_i}_{\text{growth rate}} - \underbrace{\delta N_i}_{\text{dilution rate}} \tag{90}$$

$$\frac{d[P]_i}{dt} = \underbrace{k_{e,i}[E]_i}_{\substack{\text{maximum precursor}\\ \text{synthesis rate}}} \underbrace{\frac{K_{ip,i}}{K_{ip,i}+[P]_i}}_{\substack{\text{feedback}\\ \text{inhibition}}} - \underbrace{\frac{k_{r,i}[R]_i[P]_i}{K_{mp,i}+[P]_i}}_{\substack{\text{precursor}\\ \text{consumption rate}}} - \underbrace{\Lambda_i[P]_i}_{\substack{\text{precursor}\\ \text{dilution rate}}}$$

$$- \underbrace{\frac{k_{t,i}[P]_i(1-\frac{1}{K_{ca}}\frac{[A_{ex}]_i}{[P]_i})}{K_{mp,i}+[P]_i(1+k_{tp,i}\frac{1}{K_{ca}}\frac{[A_{ex}]_i}{[P]_i})}}_{\substack{\text{reversible fermentation rate}\\ \text{with thermodynamic constrait}}} + \underbrace{\frac{k_{u,i}[E]_i[A_{ex}]_i}{K_{up,i}+[A_{ex}]_i}}_{\substack{\text{fermentation product}\\ \text{uptake rate}}} \tag{91}$$

$$\frac{d[R]_i}{dt} = \underbrace{\frac{k_{r,i}[R]_i[P]_i}{m_{r,i}(K_{mp,i}+[P]_i)}\frac{K_{ix,i}}{K_{ix,i}+[X]_i}}_{\substack{\text{ribosome}\\ \text{synthesis rate}}} - \underbrace{\Lambda_i[R]_i}_{\substack{\text{ribosome}\\ \text{dilution rate}}} \tag{92}$$

$$\frac{d[X]_i}{dt} = \underbrace{k_{x,i}\frac{K_{mp,i}}{K_{mp,i}+[P]_i}}_{\substack{\text{regulator}\\ \text{synthesis rate}}} - \underbrace{d_x[X]}_{\substack{\text{regulator}\\ \text{degradation rate}}} \tag{93}$$

$$\frac{d[A_{ex}]}{dt} = \underbrace{\frac{v_a[P](1-\frac{1}{K_{ca}}\frac{[A_{ex}]}{[P]})}{K_{mp}+[P](1+k_{ra}\frac{1}{K_{ca}}\frac{[A_{ex}]}{[P]})}}_{\substack{\text{reversible fermentation rate}\\ \text{with thermodynamic constrait}}} - \underbrace{\frac{k_u[E][A_{ex}]}{K_{mu}+[A_{ex}]}}_{\substack{\text{fermentation product}\\ \text{uptake rate}}} + \underbrace{D([A_{ex}]-[A_{ex}])}_{\substack{\text{diffusion of}\\ \text{fermentation product}}} \tag{94}$$

$$\frac{d[A_{ex}]}{dt} = \underbrace{-D([A_{ex}]-[A_{ex}])(\frac{V_cN}{V_m})}_{\substack{\text{diffusion of}\\ \text{fermentation product}}} - \underbrace{-\delta[A_{ex}]}_{\substack{\text{dilution of extracellular}\\ \text{fermentation product}}} \tag{95}$$

$$\Lambda_{biomass\ limited} = \underbrace{\frac{k_r[R][P]}{\beta(K_{mp}+[P])}}_{\substack{\text{carbon limited}\\ \text{growth rate}}} \tag{96}$$

$$\Lambda_{ATP\ limited} = \underbrace{n_pk_e[E]\frac{K_{ip}}{K_{ip}+[P]} + n_a\frac{v_a[P](1-\frac{1}{K_{ca}}\frac{[A_{ex}]}{[P]})}{K_{mp}+[P](1+k_{ra}\frac{1}{K_{ca}}\frac{[A_{ex}]}{[P]})}}_{\substack{\text{ATP limited}\\ \text{growth rate}}} \tag{97}$$

$$\Lambda = min\{\Lambda_{biomass\ limited}, \Lambda_{ATP\ limited}\} \tag{98}$$

$$[E] = \underbrace{\frac{\beta - m_r[R]}{m_e}}_{\substack{\text{metabolic protein} \\ \text{concentration}}} \tag{99}$$

[1] Surabhi Mishra and James Imlay. Why do bacteria use so many enzymes to scavenge hydrogen peroxide? *Archives of biochemistry and biophysics*, 525(2):145–160, 2012.

[2] Lauren Costa Seaver and James A Imlay. Alkyl hydroperoxide reductase is the primary scavenger of endogenous hydrogen peroxide in escherichia coli. *Journal of bacteriology*, 183(24):7173–7181, 2001.

[3] Daniel Madar, Erez Dekel, Anat Bren, Anat Zimmer, Ziv Porat, and Uri Alon. Promoter activity dynamics in the lag phase of escherichia coli. *BMC systems biology*, 7(1):136, 2013.

[4] Melanie Hillion and Haike Antelmann. Thiol-based redox switches in prokaryotes. *Biological chemistry*, 396(5):415–444, 2015.

[5] Yun-Jeong Heo, In-Young Chung, Wan-Je Cho, Bo-Young Lee, Jung-Hoon Kim, Kyoung-Hee Choi, Jin-Won Lee, Daniel J Hassett, and You-Hee Cho. The major catalase gene (kata) of pseudomonas aeruginosa pa14 is under both positive and negative control of the global transactivator oxyr in response to hydrogen peroxide. *Journal of bacteriology*, 192(2):381–390, 2010.

[6] Daniel J Hassett, Ju-Fang Ma, James G Elkins, Timothy R McDermott, Urs A Ochsner, Susan EH West, Ching-Tsan Huang, Jessie Fredericks, Scott Burnett, Philip S Stewart, et al. Quorum sensing in pseudomonas aeruginosa controls expression of catalase and superoxide dismutase genes and mediates biofilm susceptibility to hydrogen peroxide. *Molecular microbiology*, 34(5):1082–1093, 1999.

[7] Lauren Costa Seaver and James A Imlay. Hydrogen peroxide fluxes and compartmentalization inside growing escherichia coli. *Journal of bacteriology*, 183(24):7182–7189, 2001.

[8] Lewis Elwood Tomalin, Alison Michelle Day, Zoe Elizabeth Underwood, Graham Robert Smith, Piero Dalle Pezze, Charalampos Rallis, Waseema Patel, Bryan Craig Dickinson, Jürg Bähler, Thomas Francis Brewer, et al. Increasing extracellular h2o2 produces a bi-phasic response in intracellular h2o2, with peroxiredoxin hyperoxidation only triggered once the cellular h2o2-buffering capacity is overwhelmed. *Free Radical Biology and Medicine*, 95:333–348, 2016.

[9] Cheolju Lee, Soon Mi Lee, Partha Mukhopadhyay, Seung Jun Kim, Sang Chul Lee, Woo-Sung Ahn, Myeong-Hee Yu, Gisela Storz, and Seong Eon Ryu. Redox regulation of oxyr requires specific disulfide bond formation involving a rapid kinetic reaction path. *Nature Structural and Molecular Biology*, 11(12):1179, 2004.

[10] Fredrik Åslund, Ming Zheng, Jon Beckwith, and Gisela Storz. Regulation of the oxyr transcription factor by hydrogen peroxide and the cellular thiol—disulfide status. *Proceedings of the National Academy of Sciences*, 96(11):6161–6165, 1999.

[11] Ché S Pillay, Beatrice D Eagling, Scott RE Driscoll, and Johann M Rohwer. Quantitative measures for redox signaling. *Free Radical Biology and Medicine*, 96:290–303, 2016.

[12] James E Ferrell Jr and Sang Hoon Ha. Ultrasensitivity part i: Michaelian responses and zero-order ultrasensitivity. *Trends in biochemical sciences*, 39(10):496–503, 2014.

[13] James A Imlay. The molecular mechanisms and physiological consequences of oxidative stress: lessons from a model bacterium. *Nature Reviews Microbiology*, 11(7):443, 2013.

[14] Al Claiborne and I Fridovich. Purification of the o-dianisidine peroxidase from escherichia coli b. physicochemical characterization and analysis of its dual catalatic and peroxidatic activities. *Journal of Biological Chemistry*, 254(10):4245–4252, 1979.

[15] Derek Parsonage, P Andrew Karplus, and Leslie B Poole. Substrate specificity and redox potential of ahpc, a bacterial peroxiredoxin. *Proceedings of the National Academy of Sciences*, 105(24):8209–8214, 2008.

[16] Gene-Wei Li, David Burkhardt, Carol Gross, and Jonathan S Weissman. Quantifying absolute protein synthesis rates reveals principles underlying allocation of cellular resources. *Cell*, 157(3):624–635, 2014.

[17] Matthew Scott, Carl W Gunderson, Eduard M Mateescu, Zhongge Zhang, and Terence Hwa. Interdependence of cell growth and gene expression: origins and consequences. *Science*, 330(6007):1099–1102, 2010.

[18] Sheng Hui, Josh M Silverman, Stephen S Chen, David W Erickson, Markus Basan, Jilong Wang, Terence Hwa, and James R Williamson. Quantitative proteomic analysis reveals a simple strategy of global resource allocation in bacteria. *Mol. Syst. Biol.*, 11(2):784, 2015.

[19] Herbert E Kubitschek, William W Baldwin, Sally J Schroeter, and Rheinhard Graetzer. Independence of buoyant cell density and growth rate in *Escherichia coli*. *J. Bacteriol.*, 158(1):296–299, 1984.

[20] Markus Basan, Manlu Zhu, Xiongfeng Dai, Mya Warren, Daniel Sévin, Yi-Ping Wang, and Terence Hwa. Inflating bacterial cells by increased protein synthesis. *Mol. Syst. Biol.*, 11(10):836, 2015.

[21] Hans Bremer and Patrick P Dennis. Modulation of chemical composition and other parameters of the cell at different exponential growth rates. *EcoSal Plus*, 3(1), 2008.

[22] Guy Aidelberg, Benjamin D Towbin, Daphna Rothschild, Erez Dekel, Anat Bren, and Uri Alon. Hierarchy of non-glucose sugars in *Escherichia coli*. *BMC Syst. Biol.*, 8(1):133, 2014.

[23] Richard L Gourse, Tamas Gaal, Michael S Bartlett, J Alex Appleman, and Wilma Ross. rRNA transcription and growth rate-dependent regulation of ribosome synthesis in *Escherichia coli*. *Annu. Rev. Microbiol.*, 50(1):645–677, 1996.

[24] Justin J Lemke, Patricia Sanchez-Vazquez, Hector L Burgos, Gina Hedberg, Wilma Ross, and Richard L Gourse. Direct regulation of *Escherichia coli* ribosomal protein promoters by the transcription factors ppGpp and DksA. *Proc. Natl. Acad. Sci. USA*, 108(14):5712–5717, 2011.

[25] Kerli Piir, Anton Paier, Aivar Liiv, Tanel Tenson, and Ülo Maiväli. Ribosome degradation in growing bacteria. *EMBO Rep.*, 12(5):458–462, 2011.

[26] Murray P Deutscher. Degradation of stable RNA in bacteria. *J. Biol. Chem.*, 278(46):45041–45044, 2003.

[27] Stefan Klumpp, Matthew Scott, Steen Pedersen, and Terence Hwa. Molecular crowding limits translation and cell growth. *Proc. Natl. Acad. Sci. USA*, 110(42):16754–16759, 2013.

[28] Arijit Maitra and Ken A Dill. Bacterial growth laws reflect the evolutionary importance of energy efficiency. *Proc. Natl. Acad. Sci. USA*, 112(2):406–411, 2015.

[29] Allen G Marr. Growth rate of *Escherichia coli*. *Microbiol. Rev.*, 55(2):316–333, 1991.